JOURNAL OF MATERIALS SCIENCE: MATERIALS IN MEDICINE **16** (2005) 993–1001

Study of the reactivity and *in vitro* bioactivity of Sr-substituted α-TCP cements

S. JEGOU SAINT-JEAN[1,*], C. L. CAMIRÉ[2], P. NEVSTEN[1], S. HANSEN[1], M. P. GINEBRA[3]
[1]*Department of Materials Chemistry, Lund University, P.O. Box 124, SE-22100 Lund, Sweden*
E-mail: simon.jegou_saint-jean@materialkemi.lth.se
[2]*Department of Orthopaedics, Lund University Hospital, SE-22185 Lund, Sweden*
[3]*Department of Materials Science and Metallurgy, Universitat Politecnica de Catalunya, E-08028 Barcelona, Spain*

In this study the effect of strontium substitution on the hydrolysis of α-tricalcium phosphate (α-TCP) toward the formation of calcium deficient hydroxyapatite (CDHA) was investigated. For that purpose substituted α-TCP powders with 1, 5 and 10 mol% Sr substitution for Ca were synthesized by reacting at 1500 °C stoichiometric amounts of $CaCO_3$, $SrCO_3$, and $Ca_2P_2O_7$, followed by rapid quenching in air. XRD analysis of the powders revealed the presence of α-TCP (traces of β-TCP) with enlarged unit cell volume at increased Sr contents, indicating the incorporation of Sr in the crystal structure. Strontium was also incorporated in the apatite phase as revealed by XRD analysis of the set cements. The hydrolysis of milled α-SrTCP powders and a pure α-TCP (control) was monitored by isothermal calorimetry and the compressive strength of set cements was tested. The results showed a decrease in the reactivity with increasing Sr content and similar final mechanical strength within the Sr series, though lower than the control. The *in vitro* bioactivity of the set cements after soaking in simulated body fluid for 4 weeks was also tested. The formation of a bone-like apatite layer on the surface of the set cements indicated a potential *in vivo* bioactivity.

Introduction

Among the trace elements present in bone cells, strontium was found to exert beneficial effects on the osteoblastic activity. At low concentration levels (slightly higher than the physiological level), strontium administration was shown to reduce bone resorption and stimulate bone formation [1–5]. Thus, it is reasonable to expect that its presence in biomaterials can lead to a better osteointegration. With this aim, its incorporation in the calcium phosphate ceramics and cements has been the subject of much interest in the last decade [6–13].

The main and largely used constituent of the calcium phosphate ceramics and cements is hydroxyapatite (HA). Depending on the technique and the route used for the synthesis, various morphology, stoichiometry and level of crystallinity can be achieved. This provides the material with different physico-chemical properties that can affect its mechanical strength but also its biocompatibility and bioactivity. In previous works, calcium-strontium hydroxyapatites (Ca, Sr)HA have been prepared by precipitation in aqueous solution [8, 14], hydrothermal process [15], dry mechanosynthesis [11], and also by maturation of a cement made of a mixture of calcium phosphates and an acidic solution [7, 13]. *In vitro* studies on the bioactivity of (Ca, Sr)HA [2], and *in vivo* studies on (Ca, Sr)HA composite cements [10] both reported an increased bioactivity, as compared to pure CaHA. The *in vitro* studies on the (Ca, Sr)HA powders revealed a greater apatite deposition with Sr-containing HA, while the *in vivo* (Ca, Sr)HA cement study revealed an increase in the thickness of the bone layer formed at the interface bone-cement and a better osteointegration.

In this study, we investigated the effects of Sr-substitutions on the reactivity of alpha tricalcium phosphate (α-TCP). Pure α-TCP is a common reactant used in calcium phosphate cements. When it is hydrolyzed using an appropriate liquid to powder ratio, it sets giving a calcium deficient hydroxyapatite (CDHA) as a product [16–19]. The interest in using CDHA, rather than stoichiometric hydroxyapatite, lies in its resemblance to the biological apatite, in terms of structure and chemical composition. We also performed *in vitro* studies to investigate the bioactivity of the set cements, as a function of the Sr content.

*Author to whom all correspondence should be addressed.

Experimental

Preparation of the α-SrTCP powders

Stoichiometric amounts of $CaCO_3$ (Merck, p.a.), $Ca_2P_2O_7$ (prepared by firing $CaHPO_4$, Sigma #C-7263 at 1100 °C for 16 h) and $SrCO_3$ (Aldrich, p.a.) were used to reach the respective compositions 1, 5 and 10 mol% of Sr^{2+} replacing Ca^{2+} in α-TCP. The starting materials were intimately mixed in a ball mill for 15 min at 480 rpm and reacted in a Pt crucible for 4 h at 1500 °C. The powders were then quenched in air to insure the formation of the α form, and further analyzed by means of X-ray powder diffraction and scanning electron microscopy.

Hydrolysis of the α-SrTCP powders

The α-SrTCP powders were ground according to an optimized milling procedure [20] to provide a fine powder, and hydrolyzed using a 2.5 wt% Na_2HPO_4 (Merck #1.06586) accelerating solution at a liquid to powder weight ratio $L/P = 1$. The CDHA formation was monitored with an isothermal calorimeter maintained at constant temperature of 37 °C. A powder of pure α-TCP sintered at 1325 °C was milled and hydrolyzed in the same conditions and used as a control sample. Pastes of the cements ($L/P = 0.34$) were also placed in Teflon moulds (diameter = 4 mm, height = 8 mm) at a temperature of 80 °C for 4 days to insure a rapid and full hydration and these were further analyzed by means of X-ray diffraction and scanning electron microscopy.

Bioactivity of (Ca, Sr)HA

The set cements (Sr-containing samples and the control) were removed from the Teflon moulds, dried and immersed in a simulated body fluid (SBF) [21], with ion concentrations nearly equal to those of the human blood plasma, for 4 weeks at physiological temperature (37 °C) and analyzed by means of scanning electron microscopy.

X-ray diffraction measurements

X-ray diffraction analysis was performed using a Guinier focusing camera equipped with an imaging plate (Huber Imaging Plate Guinier Camera 670). Data were collected for 32000 seconds (≈9 h) using CuKα1 radiation from $2\theta = 8$ to 100°, with a 2θ-step of 0.005°. The lattice constants of the materials were determined by Rietveld refinements using the Winpow program [22], a local Windows version of the Rietveld analysis program LHPM 1 by Hill and Howard [23] and the refined crystal structures of α-TCP, β-TCP, and hydroxyapatite reported in the literature [24–26] as reference.

Isothermal calorimetry

The heat evolved during hydrolysis of α-SrTCP powders and a control was monitored using a TAM air isothermal calorimeter, which temperature was fixed at 37.0 ± 0.1 °C by circulating water from a thermostatic water bath. The powders (1.000 g) were placed in closed glass ampoules and left in the calorimeter for a few hours to acclimate to the temperature. A 2.5 wt% Na_2HPO_4 accelerating solution (1.00 ml) at 37 °C was injected into the ampoules through metal capillaries from outside the calorimeter chamber. Data (in mV) was collected every 10 s using the PICOlog software [27], and converted into Watts/mol and then integrated, resulting in a total heat of reaction in kJ/mol CDHA, $Ca_9(HPO_4)(PO_4)_5OH$, formed.

Compressive strength testing

After setting at 80 °C for 4 days, cement samples (8 per cement) were removed from the Teflon moulds and compression tested in a biaxial Instron 8511 load frame with MTS TestStar II controller. The testing was performed at room temperature with a crosshead displacement of 1 mm/min and the samples were loaded until failure.

Scanning electron microscopy

The cylindrical specimens of the set cements, soaked in SBF for 4 weeks, were dried and cleaved to analyze the thickness of new apatite layer as well as the chemical composition and morphology of the bulk apatite and the new apatite layer. X-ray energy dispersive spectrometry (XEDS) was performed on carbon coated samples at an accelerating voltage of 20 kV, using a JEOL JSM-840A instrument. The samples were then recoated by gold sputtering for imaging at 10 kV.

Results

Characterization of the cement powders and the matured cements

The examination of the X-ray diffraction patterns of the TCP powders (Fig. 1) prepared with various Sr amounts revealed the presence of the α-form (space group $P2_1/a$) with traces of β-form (space group R3c) formed during the quenching. The diffraction patterns

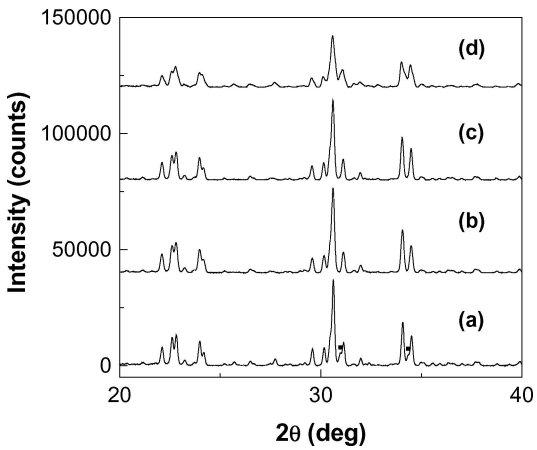

Figure 1 X-ray diffraction patterns of (a) α-Sr0%TCP, (b) α-Sr1%TCP, (c) α-Sr5%TCP, and (d) α-Sr10%TCP. The two dots represent the visible peaks of β-TCP.

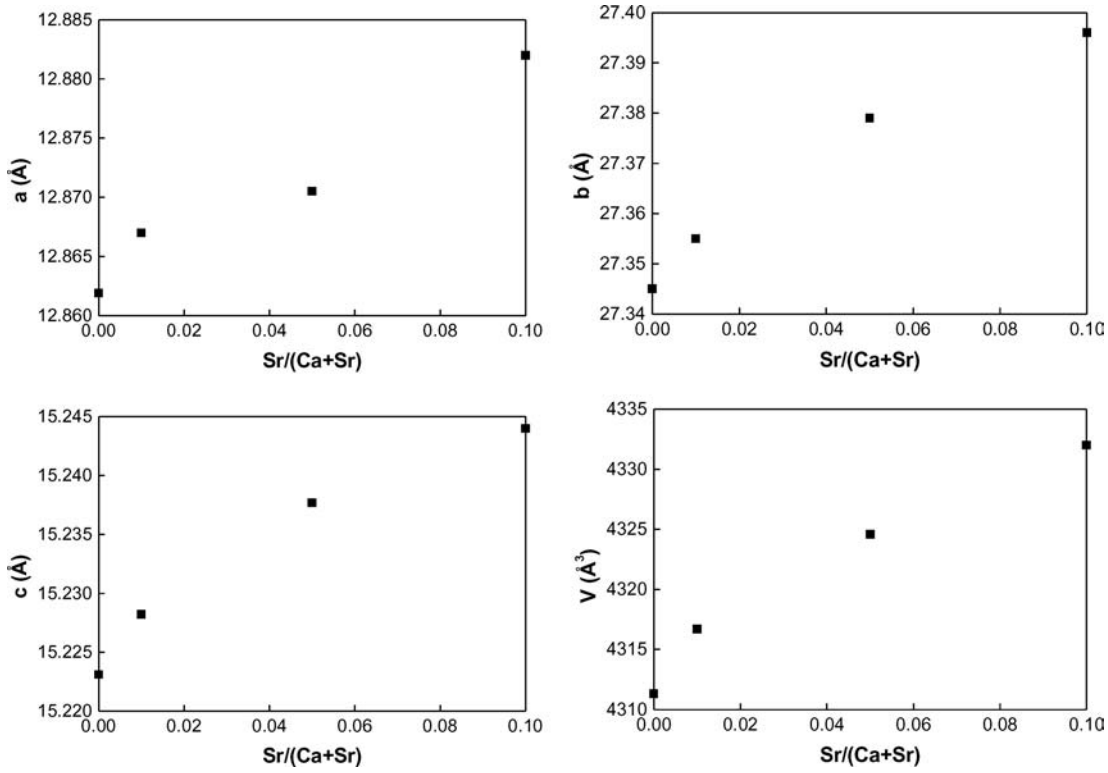

Figure 2 Variation of the lattice dimensions of α-(Ca,Sr)TCP with increasing Sr content.

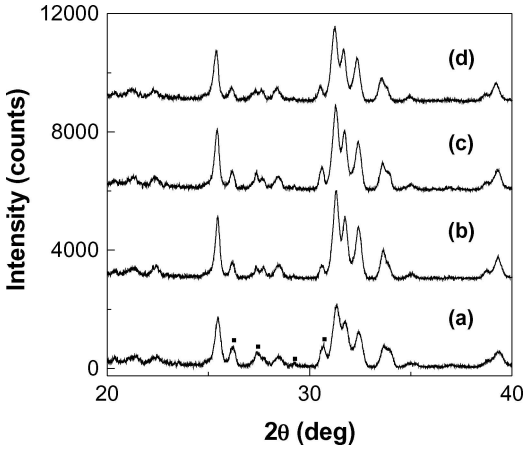

Figure 3 X-ray diffraction patterns of (a) Sr0%HA, (b) Sr1%HA, (c) Sr5%HA, and (d) Sr10%HA. The squares represent unreacted β-TCP.

of the TCP powders were slightly and continuously shifted to lower diffraction angles as increasing Sr amounts were introduced. This is characteristic of an increase of the lattice volume and indicates that strontium is incorporated in the structures (ionic radii: Sr^{2+} = 1.13 Å, Ca^{2+} = 1.00 Å). Rietveld refinement analyses performed on the powder data revealed an almost linear evolution of the lattice parameters (see Fig. 2) except for the β parameter, which did not significantly change ($\beta \approx 126.36^{\circ}$). Moreover a broadening of the peaks with increased Sr contents (Fig. 1) could be observed, indicating a reduction of the size of the TCP crystallites.

The hydrated products were well crystallized and presented diffraction patterns characteristic of an apatitic phase (space group $P6_3/m$) with small amounts of unreacted β-TCP remaining from the cement powders (Fig. 3). As with the TCP powders, a slight shift to lower 2θ angles of the diffraction peaks of the apatite phase could be observed indicating the incorporation of Sr in the crystals. The refinement results are presented in Fig. 4 and reveal an almost linear evolution of the lattice parameters. Scanning microscopy investigations showed major differences in the crystal morphology and size of the bulk apatite crystals in the (Ca, Sr)-HA series compared to the control sample. The Sr-apatites (including Sr0% apatite) in Fig. 5 consisted of radiating needle-like crystals ($\approx$2 μm long) grown from the α-TCP grains and forming a network of acicular crystal aggregates whereas the control consisted of smaller ($\approx$1 μm) and entangled plate-like crystals (see SEM pictures in Fig. 5).

Reactivity of the α-TCP powders

Different kinetics of reaction was observed for the control and the Sr series, as illustrated by the rate of heat evolution curves in Fig. 6. The hydrolysis reaction consists generally of three thermal peaks: A wetting peak corresponding to the wetting of the powder upon injection and mixing followed by two peaks associated to the hydration reaction in which α-TCP is dissolved and CDHA precipitated, all three events being more or less overlapped depending on the characteristics of the α-TCP used and the experimental conditions [19, 28–30]. In the present experiments, the wetting peaks were small and negative as a result of a difference in temperature between the fluid in the syringe and the calorimeter chamber. The hydration peaks showed the same general appearance in all the samples, with a rapid primary reaction followed by a slower final reaction. However, the occurrence and duration of the heat events varied

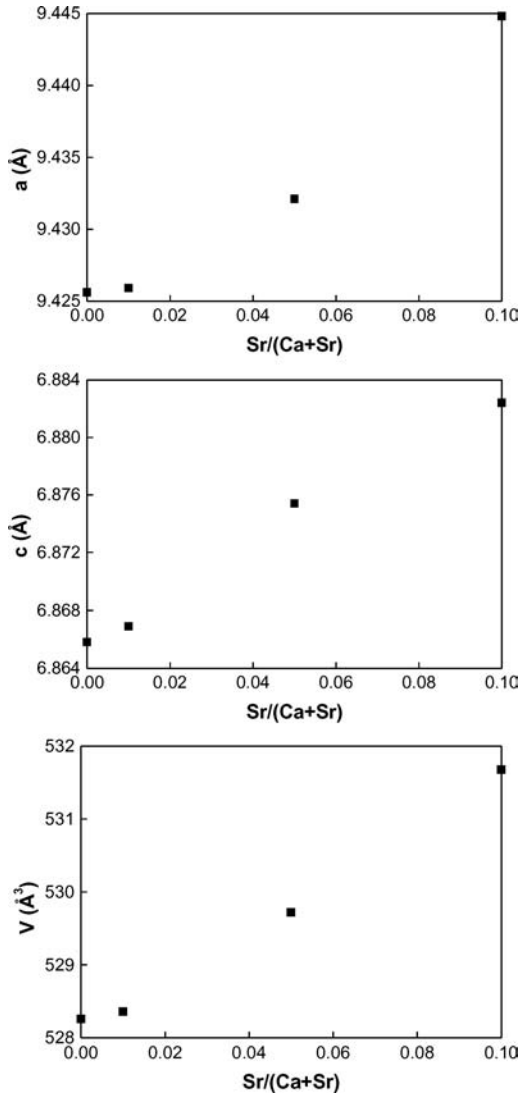

Figure 4 Variation of the lattice dimensions of (Ca,Sr)HA with increasing Sr content.

within the Sr series and from the control, the appearance of the first hydration peak being systematically delayed with increasing strontium concentrations (by about 50 min for Sr5% and 2 h 15 min for Sr10%) . Besides, the duration times for the reaction of the α-SrTCP powders were considerably prolonged, the control reaching completion after 20 h compared to about 36 h for the Sr series. The total heat produced by the formation of HA from the hydrolysis at 37 °C of α-TCP reached similar values of 128, 131, 132, 132, and 128 kJ/mol respectively for the control and the 0, 1, 5, and 10 mol% Sr containing α-TCP powders, comparable with results previously reported in the literature [19] .

Compressive strength

The compressive strength measurements of the cements fully hydrated at 80 °C (Fig. 7) revealed a rather constant strength in the Sr series, when the estimated standard deviations were taken into consideration. The strengths reached within the Sr series were still considerably lower (≈10 MPa) than for the control (≈40 MPa).

Bioactivity of (Ca, Sr)HA

After 4 weeks soaking in SBF, thin and dense layers of precipitate were formed on the surface of both the (Ca, Sr)HA samples and the control (see micrographs in Fig. 8). The layers consisted of intergrown nodules formed by small entangled plate-like apatite crystals (see micrographs in Fig. 9), similar to the bonelike apatite layers normally formed on the surface of bioactive ceramics in SBF [31]. XEDS analysis of the layers revealed that the precipitates were calcium phosphate apatite with detectable amounts of chlorine, probably incorporated in the crystal structure as chloride ions (see Fig. 10(b) and (c)). The SBF contained physiological levels of chloride, which accounted for its presence in the apatite layer. Chlorine could actually be used in our experiments as a marker to determine the apatite layer boundaries, when performing elemental mapping (Fig. 10(d) and (e)) but further investigations are necessary. In the samples with 5 and 10 Sr mol%, Sr could be detected in the apatite layer formed in SBF, indicating that the apatite cement has dissolved.

The formation of nodules was more pronounced within the Sr series compared to the control, with nodules of about 10 μm in diameter (Fig. 9). The individual crystals forming the nodules were somewhat larger in the Sr series as compared to the control, i.e. ≈1 μm compared to ≈0.5 μm. The thickness of the precipitated layers was about the same in all the samples, i.e. 16(2), 19(3), 13(2), 11(3), 16(2) μm, respectively, for: The control, Sr0%, Sr1%, Sr5%, and Sr10% (estimated standard deviations referring to the last digit given in parenthesis). The surface layer was less adhered to the surface of the set cement in the case of the control than in the Sr samples. The layer formed on the control easily fell off during the preparation of the SEM samples, whereas it was well penetrated into the pores of the bulk material in the case of the SrHA samples.

Discussion

Reactivity of α-SrTCP

SrTCP solid solutions could be prepared in the high-temperature, reactive α-form by sintering at 1500 °C, followed by rapid quenching in air. Our attempts to synthesize the strontium containing α-TCP at lower temperatures failed, despite the fact that it was possible with pure α-TCP (≈1325 °C). Also according to the reported phase diagram for the system $Sr_3(PO_4)_2$-$Ca_3(PO_4)_2$ [32], it is possible to use a temperature below 1500 °C, i.e. 1135–1264 °C from 0 to 10 mol% substitution of Sr^{2+} for Ca^{2+}. Like the choice of (i) route of synthesis, (ii) set regulating additives, and (iii) ionic substitutions, the sintering temperature also plays an important role on the reactivity of the α-TCP towards CDHA, at a given hydration temperature [33–36]. At high sintering temperatures increasing crystal growth occurs, resulting in a powder with reduced specific surface area and thus slower rate of dissolution of α-TCP and precipitation to CDHA. This is illustrated by the calorimetry data in Fig. 6, with the Sr series showing broader peaks of hydration and longer reaction times than the α-TCP sintered at 1325 °C (control). Within

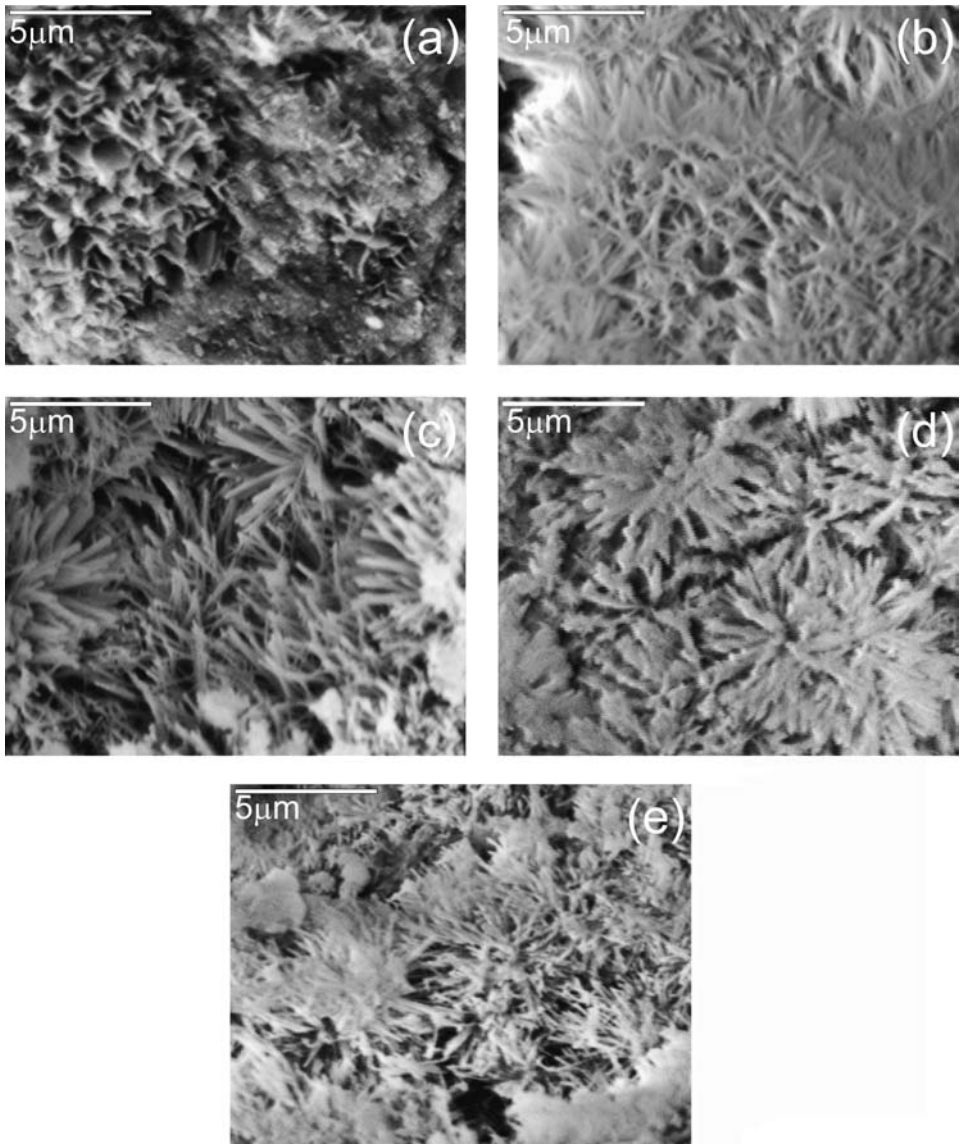

Figure 5 SEM micrographs of fracture surfaces of the hydrated α-TCP cements: (a) control (from pure α-TCP sintered at 1325 °C), (b) Sr0%HA (from pure α-TCP sintered at 1500 °C), (c) Sr1%HA, (d) Sr5%HA, and (e) Sr10%HA.

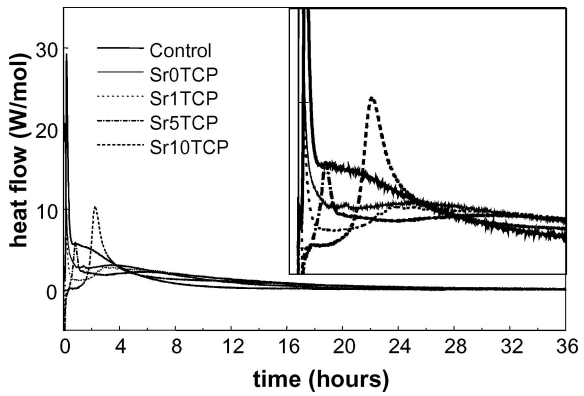

Figure 6 Isothermal calorimetry curves showing the heat evolution during hydrolysis of the control (pure α-TCP sintered at 1325 °C), and the strontium series α-Sr0%TCP (pure α-TCP sintered at 1500 °C), α-Sr1%TCP, α-Sr5%TCP, and α-Sr10%TCP. The early stage of reaction is shown in the inset (0–8 h).

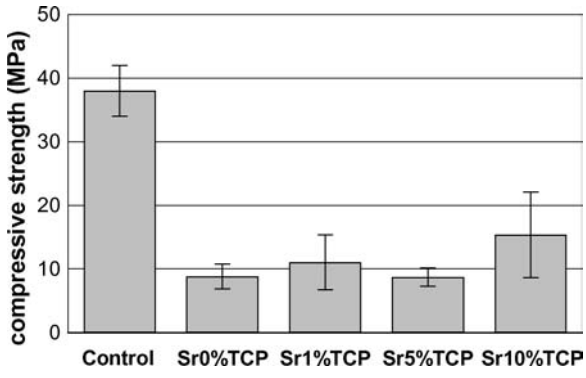

Figure 7 Compressive strength of the hydrated cement pastes.

the Sr series, increasing Sr content resulted in a retarded and slower hydration, the first peak of hydration appearing 1 to 2 h after the one of the Sr-free α-TCPs and the hydration peaks being broader. The slower rates of dissolution-precipitation observed by calorimetry might explain the difference in the shape of precipitated apatite crystals shown by the SEM pictures (Fig. 5). The more rapid dissolution of the α-TCP powder sintered at 1325 °C, and higher supersaturation of the solution with respect to apatite, caused the formation of rather small and plate-like crystals, whereas

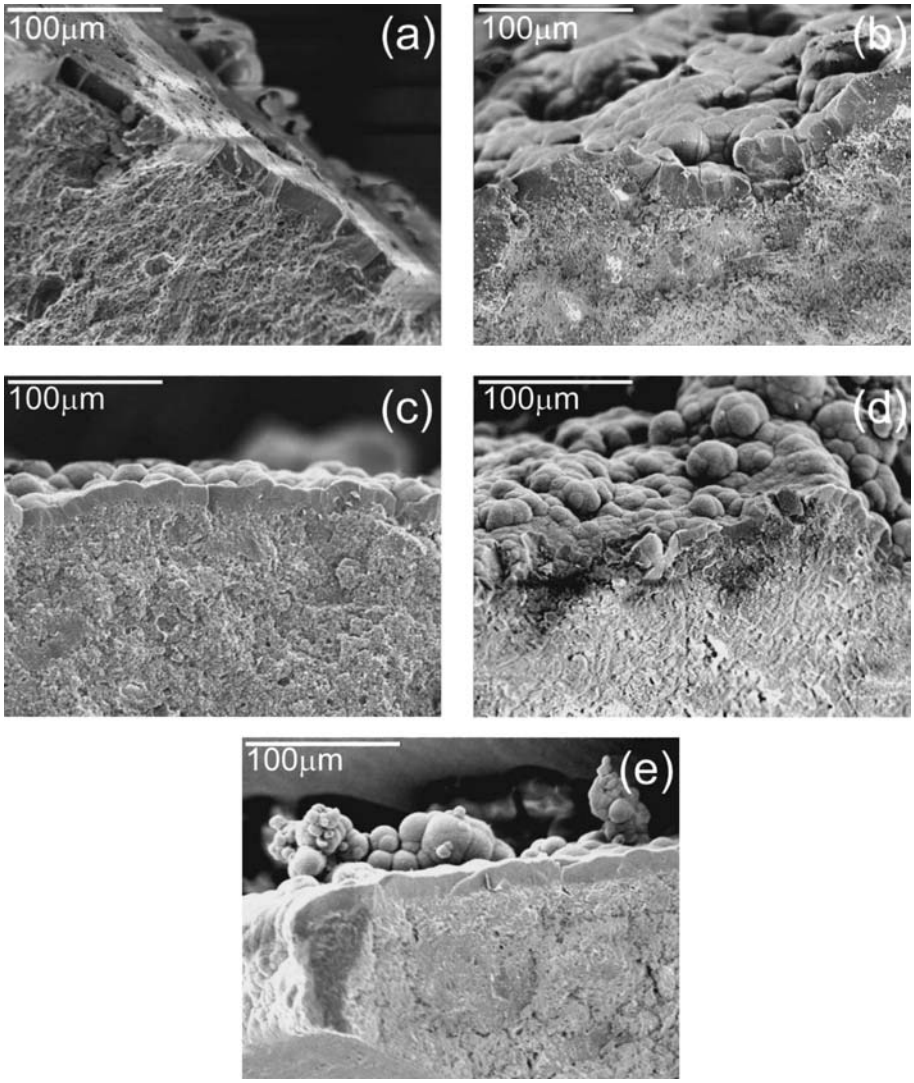

Figure 8 SEM micrographs of the apatite layer formed after 4 weeks soaking in SBF: (a) control (from pure α-TCP sintered at 1325 °C), (b) Sr0%HA (from pure α-TCP sintered at 1500 °C), (c) Sr1%HA, (d) Sr5%HA, and (e) Sr10%HA.

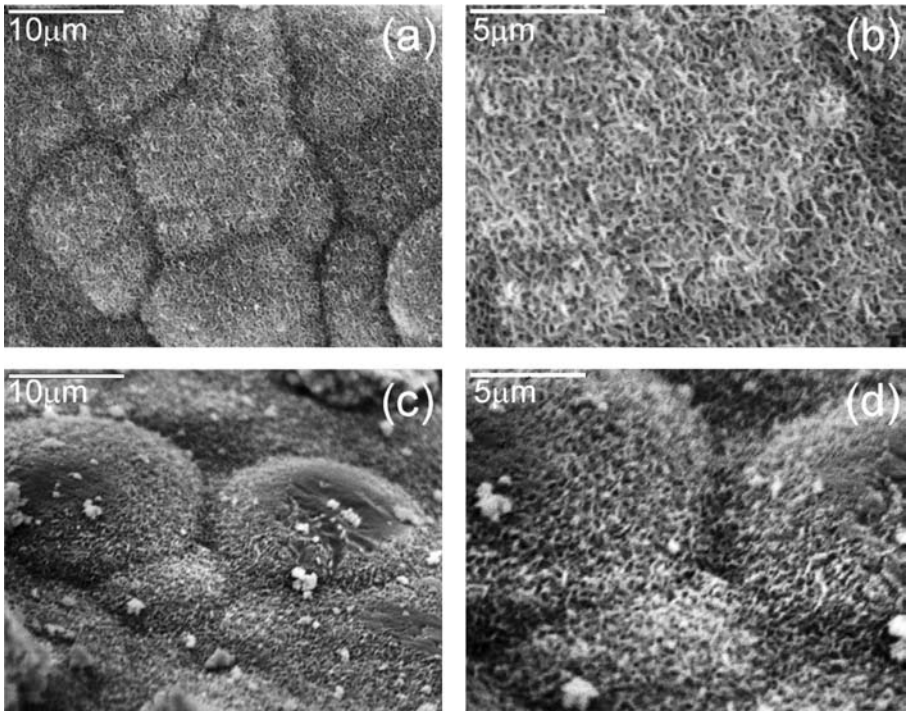

Figure 9 SEM micrographs of the HA layer formed after 4 weeks soaking in SBF: (a, b) Sr0%HA, from pure α-TCP sintered at 1500 °C, (c, d) control, from pure α-TCP sintered at 1325 °C.

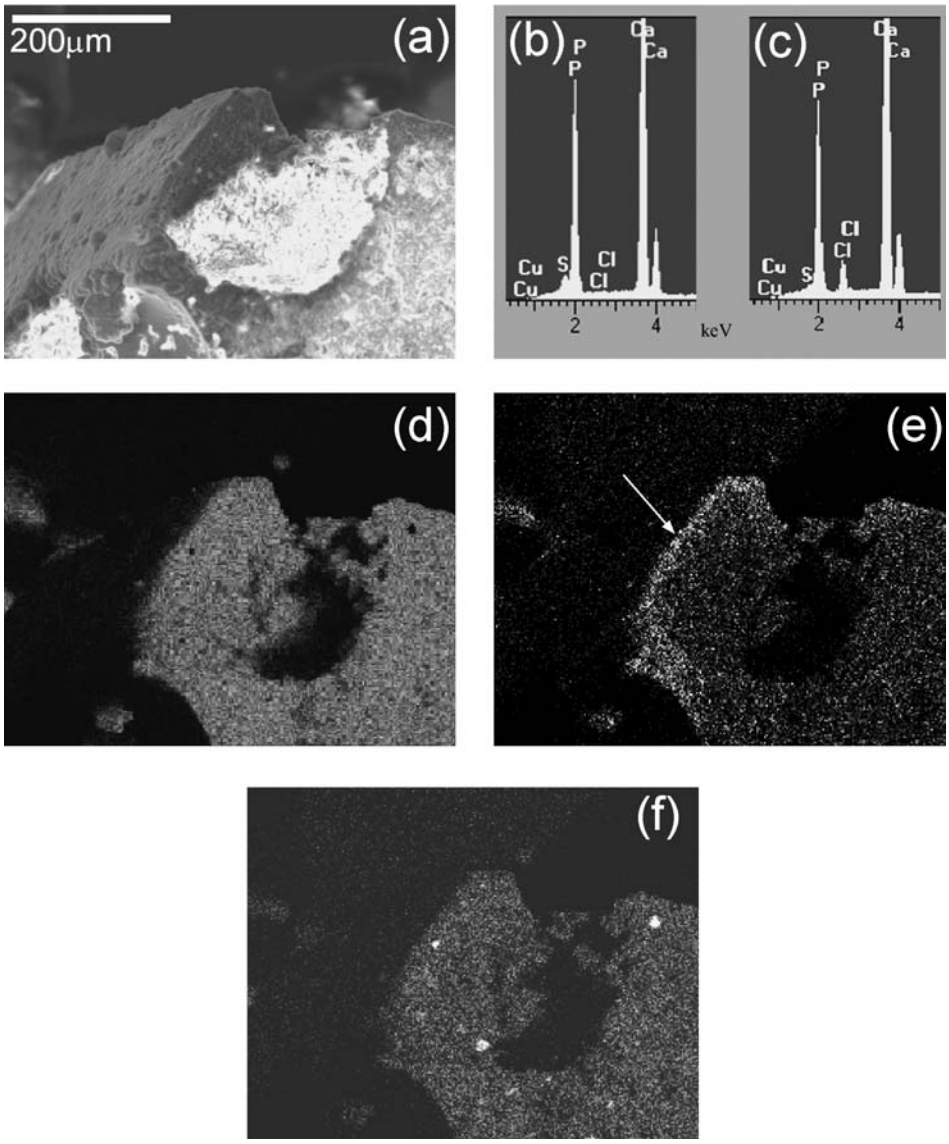

Figure 10 XEDS analysis of Sr10%HA immersed in SBF for 4 weeks: (a) Secondary electron micrograph, (b) elemental analysis of the bulk of set cement paste, (c) elemental analysis of apatite layer formed in SBF, (d) calcium X-ray map, (e) chlorine X-ray map with arrow indicating the apatite layer formed in SBF, and (f) strontium X-ray map.

the Sr series produced larger, needle-like and radiating crystals as a result of the slower reaction. The strength developed in the Sr series was lower than with the control and this can be explained by the presence of larger voids between the crystals in the Sr series.

However, shorter setting times of the SrTCPs must be obtained in order to meet clinical requirements. This might be achieved by prolonged milling of the reactants, as it has been reported in the literature [37, 38], that prolonged high energy ball milling can considerably decrease the reaction times by mechanically inducing amorphicity to the material, almost independently of the particle size, and without significantly affecting the mechanical strength.

Bioactivity of the Sr cements

The formation of an apatite layer on the surface of ceramics in SBF is an indication of its *in vivo* bioactivity, as it is well established that the formation in the body of a bone like apatite layer on the surfaces plays an essential role in the bonding of the artificial material to living bone [31, 39]. In this respect, all the set cement pastes studied here induced the formation of a bonelike apatite layer, of similar thickness, indicating that their surface is bioactive. However the morphology and texture of the apatite layers were different (Figs. 8 and 9). This further indicated a difference in the mechanisms of nucleation and growth of the apatite crystals as the result of different surface characteristics of the apatite cements. In the control, the bulk apatite consisted of small plate-like crystals tightly entangled, whereas in the Sr series it consisted of larger, needle-like crystals in radiating aggregates (Fig. 5). The small tightly entangled crystals can thus provide more nucleation sites for the precipitation of bonelike apatite crystals from SBF, than the long radiating crystals. Moreover, the larger voids created in the set Sr cement samples allowed the precipitation of new apatite to occur into the bulk, providing a better attachment of the apatite layer to the cement. The different morphology and size of the apatite crystals in both the set cements and the apatite layers formed in SBF, is thus essentially due to the effect of the sintering temperature used to synthesize the

α-TCP reactants, rather than the Sr concentration, since the apatite crystals were similar within the Sr series.

The apatite layer formed in SBF (Fig. 8) was more flat on the control sample as compared to the Sr-series, which exhibited extensive formation of nodules. The formation of nodules indicated that the nucleation of apatite from SBF was more facile on the newly formed apatite crystals, than on the original crystals, especially the larger needle-like ones.

Several *in vivo* and *in vitro* studies [1, 4] show that at low doses of strontium administration, the strontium uptake in bone may increase the bone volume by increasing the extent of bone formation sites and reducing bone resorption, without however affecting the rate of bone formation, neither altering the bone mineralization. This was found to be the result of the effect of Sr on bone cells, inducing osteoblast activity and inhibiting osteoclast activity. Additionally, the resorption *in vivo* was found to be inhibited by the stabilization of the bone apatite crystals upon Sr incorporation [40]. Contradictory results are reported in Ref. [2], actually showing that Sr incorporation in the apatite crystal structure increases its solubility in *vitro*, and that the presence of critical amounts of Sr^{2+} in aqueous solution inhibits the dissolution. However, these studies were performed *in vitro* with stoichiometric HA and SrHA crystals having thus a different chemical composition than biological apatite, which might explain the contradictory results. Nevertheless, the analysis in the same study of the apatite deposition on HA and SrHA crystals in supersaturated solution with respect to apatite, revealed a faster deposition on SrHA than on HA and inhibition of the deposition with increasing Sr^{2+} concentration in solution. In our work, none of these effects could be observed. New bone-like apatite layers were formed on all the set cements without showing significant differences in thickness.

Conclusions

Strontium containing α-tricalcium phosphate could be prepared at 1500 °C. Their reactivity toward the formation of precipitated apatite was lower than pure α-TCP prepared at lower temperature (1325 °C), and decreased with increasing strontium content. At strontium levels investigated in this study, the estimated bioactivity of the set strontium-containing apatite cements was comparable to the bioactivity of pure Ca-CDHA, making the use of strontium cements a potential alternative in the treatment of osteoporosis.

References

1. M. D. GRYNPAS, E. HAMILTON, R. CHEUNG, Y. TSOUDEROS, P. DELOFFRE, M. HOTT and P. J. MARIE, *Bone* **18** (1996) 253.
2. J. CHRISTOFFERSEN, M. R. CHRISTOFFERSEN, N. KOLTHOFF and O. BÄRENHOLDT, *ibid.* **20** (1997) 47.
3. E. ROKITA, P. H. A. MUTSAERS, J. A. QUAEDACKERS, G. TATÓN and M. J. A. DE VOIGT, *Nucl. Instr. Meth. Phys. Res.* **B 158** (1999) 412.
4. P. J. MARIE, P. AMMANN, G. BOIVIN and C. REY, *Calcif. Tissue Int.* **69** (2001) 121.
5. S. C. VERBERCKMOES, M. E. DE BROE and P. D'HAESE, *Kidney Int.* **64** (2003) 534.
6. Y. W. LI, J. C. Y. LEONG, W. W. LU, K. D. K LUK, K. M. C. CHEUNG, K. Y. CHIU and S. P. CHOW, *J. Biomed. Mater. Res.* **52** (2000) 164.
7. L. LEROUX, M. FRECHE and J. L. LACOUT, *Key. Eng. Mater.* **192–195** (2001) 235.
8. K. HAE-WONG, K. YOUNG-HAG, K. YOUNG-MIN, K. JUNG-GU and K. HYON-EE, *J. Mater. Sci. Mater. Med.* **15** (2004) 1129.
9. F. ZHAO, W. W. LU, K. D. K LUK, K. M. C. CHEUNG, C. T WONG, J. C. Y. LEONG and K. D. YAO, *J. Biomed. Mater. Res.* **69B** (2004) 79.
10. C. T. WONG, W. W. LU, W. K. CHAN, K. M. C. CHEUNG, K. D. K. LUK, D. S. LU, A. B. M. RABIE, L. F. DENG and J. C. Y. LEONG, *ibid.* **68A** (2004) 513.
11. H. EL BRIAK-BEN ABDESLAM, B. PAUVERT, A. TEROL and P. BOUDEVILLE, *Key Eng. Mater.* **254–256** (2004) 103.
12. S. JEGOU SAINT-JEAN, C. L. CAMIRE, C. MOCHALES-PALAU, S. HANSEN, I. MC CARTHY and M.P. GINEBRA, in Transactions 7th World Biomaterials Congress, Sydney, May 2004. Brunswick Lower: Australian Society for Biomaterials (2004) p. 1438.
13. D. GUO, K. XU, X. ZHAO and Y. HAN, *Biomater.* **26** (2005) 4073.
14. T. ISHIKAWA, H. SAITO, A. YASUKAWA and K. KANDORI, *J. Chem. Soc. Faraday Trans.* **89** (1993) 3821.
15. B. DONAZZON, G. DECHAMBRE and J. L. LACOUT, *Ann. Chim. Sci. Mat.* **23** (1998) 53.
16. H. MONMA, S. UENO and T. KANAZAWA, *J. Chem. Technol. Biol.* **31** (1981) 15.
17. M. P. GINEBRA, E. FERNANDEZ, M. G. BOLTONG, F. C. M. DRIESSENS, J. GINEBRA, E. A. P. DE MAEYER, R. M. H. VERBEECK and J. A. PLANELL, *J. Dent. Res.* **76** (1997) 905.
18. Y. LI, X. ZHANG and K. DE GROOT, *Biomater.* **18** (1997) 737.
19. K. S. TENHUISEN and P. W. BROWN, *ibid.* **19** (1998) 2209.
20. M. P. GINEBRA, E. FERNANDEZ, F. C. M. DRIESSENS, M. G. BOLTONG and J. A. PLANELL, In Bioceramics 10: Proceedings of the 10th International Symposium on Ceramics in Medicine (1997) p. 481.
21. A. OYANE, H. M. KIM, T. FURUYA, T. KOKUBO, T. MIYAZAKI and T. NAKAMURA, *J. Biomed. Mater. Res.* **65A** (2003) 188.
22. Winpow, program for Rietveld refinement, K. STÅHL, Technical University of Denmark, Lyngby.
23. R. J. HILL and C. J. HOWARD, Australian Atomic Energy Commission (now ANSTO), (1986) Report M112, Lucas Heights Research Laboratories, New South Wales, Australia.
24. M. MATHEW, L. W. SCHROEDER, B. DICKENS and W. E. BROWN, *Acta Crystallogr.* **B33** (1977) 1325.
25. B. DICKENS, L. W. SCHROEDER and W. E. BROWN, *J. Solid State Chem.* **10** (1974) 232.
26. M. I. KAY, R. A. YOUNG and A. S. POSNER, *Nature* **204** (1964) 1050.
27. Pico Technology Limited, UK.
28. C. DURUCAN and P. W. BROWN, *J. Mater. Sci. Mater. Med.* **11** (2000) 365.
29. C. DURUCAN and P. W. BROWN, *J. Amer. Ceram. Soc.* **85** (2002) 2013.
30. C. L. CAMIRE, S. JEGOU SAINT-JEAN, I. MCCARTHY, S. HANSEN and L. LIDGREN, *J. Appl. Biomater. Biomech* (Submitted to).
31. T. KOKUBO, *Biomaterials* **12** (1991) 155.
32. J. F. SARVER, M. V. HOFFMAN and F. A. HUMMEL, *J. Electrochem. Soc.* **108** (1961) 1103.
33. C. DURUCAN and P. W. BROWN, *J. Mater. Sci.* **37** (2002) 963.
34. M. P. GINEBRA, M. G. BOLTONG, E. FERNANDEZ, J. A. PLANELL and F. C. M. DRIESSENS, *J. Mater. Sci. Mater. Med.* **6** (1995) 857.

35. I. KHAIROUM, M. G. BOLTONG, F. C. M. DRIESSENS and J. A. PLANELL, *Biomaterials* **18** (1997) 1535.
36. E. FERNANDEZ, M. G. BOLTONG, M. P. GINEBRA, , O. BERMUDEZ, F. C. M. DRIESSENS and J. A. PLANELL, *Clin. Mater.* **16** (1994) 99.
37. U. GBURECK, J. E. BARRALET, L. RADU, H. G. KLINGER and R. THULL, *J. Amer. Ceram. Soc.* **87** (2004) 1126.
38. C. L. CAMIRE, U. GBUREK, W. HIRSIGER and M. BOHNER, *Biomater.* **26** (2004) 2787.
39. W.Q. YAN, T. NAKAMURA, M. KOBAYASHI, H. M. KIM, F. MIYAJI and T. KOKUBO, *J. Biomed. Mater. Res.* **37** (1997) 267.
40. M. E. J. CURZON and P. C. SPECTOR, *Caries Res.* **17** (1983) 249.

Received 13 April
and accepted 28 June 2005